Biologically Inspired Self-motion Estimation using the Fusion of Airspeed and Optical Flow

Adam J. Rutkowski, Roger D. Quinn, Mark A. Willis

Abstract— **The problem of determining the self-motion of an autonomous aerial vehicle using onboard sensors is of interest to both engineers and biologists. Engineers typically use some combination of a global positioning system receiver, inertial measurement units, and optical sensors to estimate self motion. Biological systems also possess visual and inertial sensors. Airspeed sensors are also available to both engineering and biological system. The method of self-motion estimation proposed in this paper is to fuse optical flow with airspeed information. Simulation results indicate that this approach can be used to calculate ground speed and wind speed while moving.**

Keywords-sensor fusion, biological systems, optical flow

I. INTRODUCTION

The problem of determining the self-motion of an autonomous aerial vehicle using onboard sensors is of interest to both engineers and biologists. Engineers use information from sensors onboard unmanned aerial vehicles (UAVs) and missiles to navigate to a target. Biologists are interested in understanding how insects determine self-motion to accomplish similar tasks. Many insect behaviors are based on the insect being able to estimate its self-motion.

Many approaches for estimating self-motion of an aerial vehicle using onboard sensors have been proposed or studied. In biological systems, distance estimation has only been shown to occur in situations that allow an interaction among the visual, proprioceptive, and vestibular systems [4]. Likewise, in engineering systems, various different sensor modalities are integrated to determine an estimate of self-motion. Most of these algorithms fall into one of the following groups: integration of a Global Positioning System (GPS) receiver and an Inertial Measurement Unit (IMU), integration of an IMU and vision sensor, and integration of vision and range finding [1][2][3]. Integration of GPS and IMU is the most common. Each type of sensor has its advantages and disadvantages as viewed from both engineering and biological perspectives.

This work was supported in part by the U.S. Air Force under grant F08630-03-1-0003 and by the Ohio Space Grant Consortium.

Adam J. Rutkowski is with the Department of Mechanical and Aerospace Engineering, Case Western Reserve University, Cleveland, OH 44106 USA (email: adam.rutkowski@case.edu).

Roger D. Quinn is with the Department of Mechanical and Aerospace Engineering, Case Western Reserve University, Cleveland, OH 44106 USA (email: rdq@case.edu).

Mark A. Willis is with the Department of Biololgy, Case Western Reserve University, Cleveland, OH 44106 USA (email: maw27@case.edu).

GPS is an attractive solution to engineers because it provides absolute position information. However, GPS can be jammed and is not usable indoors. GPS is not available to biological systems, yet there are several behaviors exhibited by animals that indicate that they can estimate their self-motion.

In biological systems, the eyes play an important part in navigation. Engineers have used cameras in place of eyes to aid in navigation. Biologists have shown that insects use optical flow to detect and help quantify their self-motion [5]. Optical flow is a measure of the apparent visual motion of an object. It can be used to determine rotational velocity by itself and it can be used in tandem with range information to determine translational velocity because translational velocity is scaled with respect to the distance to objects in the visual environment.

Distance to objects can be estimated using stereo vision or a laser range finder. Insects do not have a system equivalent to a laser range finder and it has been demonstrated that stereo vision in insects is only accurate up to a distance of a few centimeters [5]. Therefore, insects must determine their self motion by some other combination of sensors.

Inertial sensors are used to aid in navigation of both biological and engineered systems. Engineers use gyroscopes to measure angular velocities and accelerometers to measure linear accelerations. The halteres of *Diptera*, the true flies, function as gyroscopes to measure spatial rotations of the fly's body [6]. It was found that flies use halteres to detect angular motions that are too fast to measure with their visual system. The halteres are not sensitive enough to measure slow rotations, so in this case, vision is favored.

The problem of wind speed estimation is also of interest to both biologists and engineers. For example, wind speed estimation is particularly important to insects when they are tracking pheromone plumes. In general, when an insect detects a pheromone, it wants to fly upwind toward the source of the pheromone (a potential mate). This strategy is known as anemotaxis [7]. Engineers use wind speed estimation for pollution tracking, fire prevention, and weather prediction using UAVs [8].

It is not possible to measure wind speed directly while moving. One way to estimate wind speed is through the fusion of thrust and optical flow information. This strategy has been hypothesized for moths tracking pheromone plumes [9]. Another strategy is to use a knowledge of self-dynamics, control inputs (thrust and control surface deflections), and inertial measurements [8].

This paper proposes fusing optical flow with airspeed information to estimate self-motion of an aerial vehicle. Both engineered and biological systems have sensors that are capable of measuring the velocity of the air relative to themselves. In an engineered system, pitot tubes are typically used to measure airspeed, but they respond slowly and only provide the component of the airspeed vector aligned with the axis of the vehicle. A set of orthogonal hot wires or acoustic Doppler anemometers could provide directional airspeed information and respond much more quickly. The deflection of wind sensitive hairs on the antenna of insects provides information on both airspeed and direction. The distal segments of the antennae are covered with hair-like sensors and hence are probably the main wind sensitive region of an insect [10].

II. METHODS

Figure 1 shows the scenario for which the self-motion estimation algorithm is designed. A vehicle (or insect) flies over level ground at a variable altitude h. A camera is mounted on the vehicle such that the camera points directly downward at all times. A Cartesian coordinate system is fixed to the camera such that the positive z-axis is pointed directly away from the ground and the positive x-axis is aligned with the longitudinal axis of the vehicle. The vehicle moves with a true ground speed, or speed relative to the ground, of $\mathbf{v}_g$. The vehicle is constrained to rotate only about the z-axis with an angular velocity of ω_z. Wind is present with vector velocity $\mathbf{w}$ relative to the ground. Sensors onboard the vehicle measure a true airspeed, or speed relative to the surrounding air, of $\mathbf{v}_a$. Since the vehicle is assumed to not rotate about the x or y axes, the camera remains pointed downward at all times.

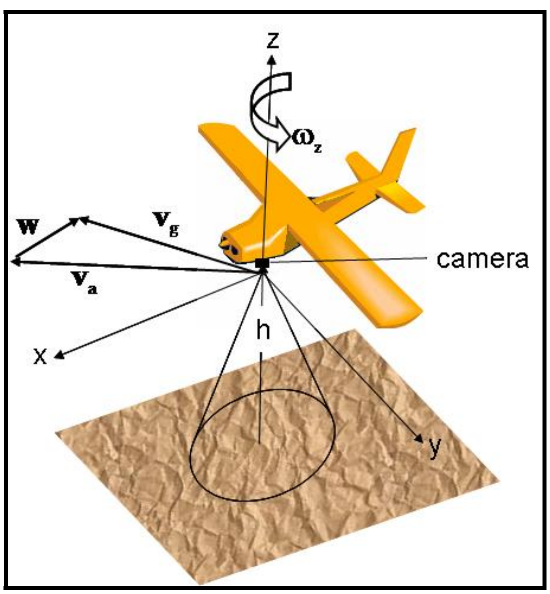

Figure 1. Schematic of the relationship between ground speed ($\mathbf{v}_g$), airspeed ($\mathbf{v}_a$), and wind speed ($\mathbf{w}$)

For simplicity, it is assumed that airspeed and optical flow are sampled simultaneously and at a constant rate. The time between samples is Δt. It is also assumed that optical flow information is obtained instantaneously at each sampling time. Let t_i represent the time at which the i^{th} sample of data is taken. Vectors $\mathbf{v}_a(t_i)$ $\mathbf{w}(t_i)$, and $\mathbf{v}_g(t_i)$ are vectors at time t_i. The first, second, and third components of these vector are the x-component, y-component, and z-component, respectively. The following vector equation relates airspeed, wind speed, and ground speed at time t_i.

$$\mathbf{v}_a(t_i) = \mathbf{v}_g(t_i) - \mathbf{w}(t_i) \quad (1)$$

The self-motion estimation technique developed here is designed to work directly with the optical flow algorithm developed by Srinivasan [11]. His algorithm provides translational optical flow data along the x and y axes and rotational optical flow data about the z axis. Translational optical flow in the z direction can be computed from looming, or the apparent motion of the image toward or away from the camera [12]. Translational optical flow as measured by the camera is quantified in pixels/second. Since each pixel in an image taken by the camera represents a certain angular displacement, the motion of the visual world can be quantified in radians/second by multiplying the raw optical flow data by a constant scale factor to yield the translational optical flow vector $\mathbf{v}_o(t_i)$ in radians per second. If $h(t_i)$ is the true height above the visual world at time t_i, then the ground speed is related to optical flow by (2).

$$\mathbf{v}_g(t_i) = h(t_i) \cdot \mathbf{v}_o(t_i) \quad (2)$$

Substituting (2) into (1) gives the relationship between airspeed, wind speed, and optical flow.

$$\mathbf{v}_a(t_i) = h(t_i) \cdot \mathbf{v}_o(t_i) - \mathbf{w}(t_i) \quad (3)$$

The goal of our algorithm is to first determine an estimate of the altitude, which will be denoted as $\hat{h}(t_i)$. Once the height is estimated, an estimate of the wind speed, $\hat{\mathbf{w}}(t_i)$, can be obtained using (4), which is simply (3) rewritten with $\hat{h}(t_i)$ substituted for $h(t_i)$ and $\hat{\mathbf{w}}(t_i)$ substituted for $\mathbf{w}(t_i)$.

$$\hat{\mathbf{w}}(t_i) = \hat{h}(t_i) \cdot \mathbf{v}_o(t_i) - \mathbf{v}_a(t_i) \quad (4)$$

Notice that if $\mathbf{v}_a(t_i)$ and $\mathbf{v}_o(t_i)$ are known, equation (4) cannot be solved for $\hat{\mathbf{w}}(t_i)$ and $\hat{h}(t_i)$, in other words, the equation is underdetermined. By adding constraints on the wind velocity over a short time period, we can solve for $\hat{\mathbf{w}}(t_i)$ and $\hat{h}(t_i)$ using airspeed and optical flow information from the current *and previous* time steps.

The first step is to convert all vectors from previous time steps into the coordinate frame of the current time step. This is done using rotation matrices. A coordinate system fixed to the camera rotates through an angle $\Delta\theta(t_i)$ when moving from an orientation at time t_{i-1} to an orientation at time t_i. The differential angular displacement $\Delta\theta(t_i)$ can be calculated as $\omega_{oz}(t_i)\Delta t$, where $\omega_{oz}(t_i)$ is the angular velocity of the camera about the z-axis as calculated by the optical flow algorithm. The rotation matrix, $\mathbf{C}(t_i,t_{i-1})$ that transforms vectors from the reference frame at time t_{i-1} to the reference frame at time t_i is given by (5).

$$\mathbf{C}(t_i,t_{i-1}) = \begin{bmatrix} \cos(\omega_{oz}(t_i)\Delta t) & \sin(\omega_{oz}(t_i)\Delta t) & 0 \\ -\sin(\omega_{oz}(t_i)\Delta t) & \cos(\omega_{oz}(t_i)\Delta t) & 0 \\ 0 & 0 & 1 \end{bmatrix} \quad (5)$$

Velocity vectors from previous time steps can be transformed into the reference frame of the current time step using (6), where $\mathbf{v}_{/t_i}(t_{i-j})$ represents a generic velocity vector at time t_{i-k} relative to the reference frame at time t_i.

$$\mathbf{v}_{/t_i}(t_{i-j}) = \mathbf{C}(t_i,t_{i-1})\cdots\mathbf{C}(t_{i-j+1},t_{i-j})\mathbf{v}_{/t_{i-j}}(t_{i-j}) \quad (6)$$

The velocity vector of **v** in (6) can be replaced with either $\mathbf{v}_o$ or $\mathbf{v}_a$ to transform all measured quantities into the current reference frame. From this point onward, the '$/t_i$' in the subscript will be dropped and it will be assumed that the airspeed and optical flow data has already been transformed to the current reference frame.

If we know the height at t_{i-1}, then the height at the previous time step t_i can be estimated with the trapezoidal rule given in (7). Let $\hat{h}(t,t_i)$ be the height at time t estimated at some future time t_i. Likewise, let $\hat{v}_{gz}(t,t_i)$ be the z component of the ground speed vector at time t estimated at time t_i.

$$\begin{aligned}\hat{h}(t_{i-1},t_i) &= \hat{h}(t_i,t_i) - \tfrac{1}{2}(\hat{v}_{gz}(t_{i-1},t_i) + \hat{v}_{gz}(t_i,t_i))(\Delta t) \\ &= \hat{h}(t_i,t_i) - \tfrac{1}{2}(v_{oz}(t_{i-1})\hat{h}(t_{i-1},t_i) + v_{oz}(t_i)\hat{h}(t_i,t_i))(\Delta t)\end{aligned} \quad (7)$$

Equation (7) can be rearranged to solve for $\hat{h}(t_{i-1},t_i)$ explicitly in terms of $\hat{h}(t_i,t_i)$ in the following way.

$$\hat{h}(t_{i-1},t_i) = \frac{1-\frac{1}{2}v_{oz}(t_i)(\Delta t)}{1+\frac{1}{2}v_{oz}(t_{i-1})(\Delta t)}\hat{h}(t_i,t_i) = s_h(t_{i-1},t_i)\hat{h}(t_i,t_i) \quad (8)$$

A recursive rule for s_h is defined by (9).

$$\begin{aligned} s_h(t_{i-k},t_i) &= \frac{1-\frac{1}{2}v_{oz}(t_{i-k+1})(\Delta t)}{1+\frac{1}{2}v_{oz}(t_{i-k})(\Delta t)} s_h(t_{i-k+1},t_i) \\ s_h(t_i,t_i) &= 1 \end{aligned} \quad (9)$$

We can now write

$$\begin{bmatrix} \hat{h}(t_i,t_i) \\ \hat{h}(t_{i-1},t_i) \\ \vdots \\ \hat{h}(t_{i-n+1},t_i) \end{bmatrix} = \begin{bmatrix} 1 \\ s_h(t_{i-1},t_i) \\ \vdots \\ s_h(t_{i-n+1},t_i) \end{bmatrix} \hat{h}(t_i,t_i) = \mathbf{S}_h(t_i,n)\cdot\hat{h}(t_i,t_i) \quad (10)$$

Let $\hat{\mathbf{w}}(t,t_i,h)$ denote an estimate at time t_i of the wind speed vector at time $t<t_i$. This can now be calculated from $\hat{h}(t_i)$. For consistency, define $\hat{\mathbf{w}}(t_i)=\hat{\mathbf{w}}(t_i,t_i,\hat{h}(t_i))$. Let e_j represent a principle direction, where e_1 is the x-direction, e_2 is the y-direction and e_3 is the z-direction. We will later see that treating each directional component of $\hat{\mathbf{w}}(t,t_i,h)$ separately is beneficial. Given an estimate of the height $\hat{h}(t_i)$, the wind speed over n time steps can be estimated using (11).

$$\begin{bmatrix} \hat{w}_{e_j}(t_i,t_i,\hat{h}(t_i)) \\ \hat{w}_{e_j}(t_{i-1},t_i,\hat{h}(t_i)) \\ \vdots \\ \hat{w}_{e_j}(t_{i-n+1},t_i,\hat{h}(t_i)) \end{bmatrix} = \begin{bmatrix} v_{oe_j}(t_i) \\ v_{oe_j}(t_{i-1})\cdot s_h(t_{i-1},t_i) \\ \vdots \\ v_{oe_j}(t_{i-n+1})\cdot s_h(t_{i-n+1},t_i) \end{bmatrix}\hat{h}(t_i) - \begin{bmatrix} v_{ae_j}(t_i) \\ v_{ae_j}(t_{i-1}) \\ \vdots \\ v_{ae_j}(t_{i-n+1}) \end{bmatrix} \quad (11)$$

$$j = 1,2,3$$

We can condense the form of (11) using (12) and (13), where **V** is a generic velocity vector.

$$\mathbf{V}_{e_1}(t_i,n) = \begin{bmatrix} v_{e_1}(t_i) \\ v_{e_1}(t_{i-1}) \\ \vdots \\ v_{e_1}(t_{i-n+1}) \end{bmatrix} \quad (12)$$

$$\mathbf{V}(t_i,n) = \begin{bmatrix} \mathbf{V}_{e_1}(t_i,n) \\ \mathbf{V}_{e_2}(t_i,n) \\ \mathbf{V}_{e_3}(t_i,n) \end{bmatrix} \quad (13)$$

Applying (10), (12), and (13) to (11) results in the compact form given in (14), where the diag() operation creates a diagonal matrix from the elements of the vector argument.

$$\hat{\mathbf{W}}(t_i,\hat{h}(t_i),n) = \mathrm{diag}(\mathbf{V}_o(t_i,n))\begin{bmatrix} \mathbf{S}_h(t_i,n) \\ \mathbf{S}_h(t_i,n) \\ \mathbf{S}_h(t_i,n) \end{bmatrix}\hat{h}(t_i) - \mathbf{V}_a(t_i,n) \quad (14)$$

Let $\breve{\mathbf{w}}(t,t_i,\mathbf{A})$ be a polynomial approximation to the true wind velocity $\mathbf{w}(t)$ using the coefficients in the matrix **A** and using time t_i as a reference. The value of $\breve{\mathbf{w}}(t,t_i,\mathbf{A})$ is given by (15), where m is the degree of the polynomial.

$$\breve{\mathbf{w}}(t,t_i,\mathbf{A}) = \mathbf{a}_0 + \mathbf{a}_1(t-t_i) + \ldots + \mathbf{a}_m(t-t_i)^m \tag{15}$$

Let the coefficients be organized into a matrix **A** as given by (16).

$$\mathbf{A} = \begin{bmatrix} \mathbf{a}_0{}^{\mathsf{T}} \\ \mathbf{a}_1{}^{\mathsf{T}} \\ \vdots \\ \mathbf{a}_m{}^{\mathsf{T}} \end{bmatrix} = \begin{bmatrix} a_{0e_1} & a_{0e_2} & a_{0e_3} \\ a_{1e_1} & a_{1e_2} & a_{1e_3} \\ \vdots & \vdots & \vdots \\ a_{me_1} & a_{me_2} & a_{me_3} \end{bmatrix} \tag{16}$$

The polynomial approximation to the wind speed vector over n time steps can be estimated using (11), where **T** is a Vandermonde matrix in time given in (18) and the superscript T indicates the transpose operation.

$$\breve{\mathbf{W}}_{e_j}(t_i,\mathbf{A},n) = \begin{bmatrix} \breve{w}_{e_j}(t_i,t_i,\mathbf{A}) \\ \breve{w}_{e_j}(t_{i-1},t_i,\mathbf{A}) \\ \vdots \\ \breve{w}_{e_j}(t_{i-n+1},t_i,\mathbf{A}) \end{bmatrix} = (\mathbf{TA})^{\mathsf{T}} \tag{17}$$

$$\mathbf{T} = \begin{bmatrix} 1 & 0 & 0 & \cdots & 0 \\ 1 & \Delta t & (\Delta t)^2 & \cdots & (\Delta t)^m \\ 1 & 2\Delta t & (2\Delta t)^2 & \cdots & (2\Delta t)^m \\ \vdots & \vdots & \vdots & & \vdots \\ 1 & (n-1)\Delta t & ((n-1)\Delta t)^2 & \ldots & ((n-1)\Delta t)^m \end{bmatrix} \tag{18}$$

The parameters $\breve{\mathbf{W}}_{e_1}(t_i,\mathbf{A},n)$, $\breve{\mathbf{W}}_{e_2}(t_i,\mathbf{A},n)$, and $\breve{\mathbf{W}}_{e_3}(t_i,\mathbf{A},n)$ can be condensed into a single vector $\breve{\mathbf{W}}(t_i,\mathbf{A},n)$ of length 3n using (13).

The height can now be estimated by minimizing the sum of the squares of the difference between estimates of the wind speed and a polynomial of degree m approximating the wind speed over the time interval (t_{i-n+1},t_i). This is equivalent to finding values for $\hat{h}(t_i)$ and **A** that solve the minimization problem of (19), where $\|\cdot\|_2$ represents the 2-norm or Euclidean norm. It is necessary that m<n.

$$\min_{\hat{h},\mathbf{A}} \left(\left\| \hat{\mathbf{W}}(t_i,\hat{h},n) - \breve{\mathbf{W}}(t_i,\mathbf{A},n) \right\|_2^2 \right) \tag{19}$$

Assume for the moment that the estimate of the height $\hat{h}(t_i)$ has already been calculated. The coefficients in the matrix **A** that solve the minimization problem of (19) are determined from (20), where the superscript + indicates the pseudoinverse operation.

$$\begin{bmatrix} \mathbf{a}_{e_1} \\ \mathbf{a}_{e_2} \\ \mathbf{a}_{e_3} \end{bmatrix} = \begin{bmatrix} \mathbf{T} & \mathbf{0} & \mathbf{0} \\ \mathbf{0} & \mathbf{T} & \mathbf{0} \\ \mathbf{0} & \mathbf{0} & \mathbf{T} \end{bmatrix}^{+} (\mathbf{V}_o(t_i)\hat{h}(t_i) - \mathbf{V}_a(t_i)) \tag{20}$$

We can define vectors **L** and **R** as follows, where **I** is an (m+1)×(m+1) identity matrix.

$$\begin{aligned} \mathbf{L}_{e_j} &= (\mathbf{TT}^{+} - \mathbf{I})\mathrm{diag}(\mathbf{V}_{oe_j})\mathbf{S}_h \\ \mathbf{R}_{e_j} &= (\mathbf{TT}^{+} - \mathbf{I})\mathbf{V}_{ae_j} \end{aligned} \tag{21}$$

The minimization problem can be solved efficiently by first taking the reduced QR factorization of **T**.

$$\mathbf{T} = \mathbf{Q}_T\mathbf{R}_T \tag{22}$$

Since **T** is invariant with time, the QR factorization of **T** can be performed during the initialization of the algorithm. Substituting (22) into (21) and simplifying gives the equations in (23).

$$\begin{aligned} \mathbf{L}_{e_j} &= (\mathbf{Q_T Q_T}^{\mathsf{T}} - \mathbf{I})\mathrm{diag}(\mathbf{V}_{oe_j})\mathbf{S}_h \\ \mathbf{R}_{e_j} &= (\mathbf{Q_T Q_T}^{\mathsf{T}} - \mathbf{I})\mathbf{V}_{ae_j} \end{aligned} \tag{23}$$

The form of (23) can be condensed using (13). By substituting (20) back into (17) then into (19), then using the parameters defined in (23), the minimization problem takes the form of (24).

$$\min_{\hat{h}(t_i)} \left\| \mathbf{L}\hat{h}(t_i) - \mathbf{R} \right\|_2^2 \tag{24}$$

The solution of Equation (24) is given (25).

$$\hat{h}(t_i) = \frac{\mathbf{L}^{\mathsf{T}}\mathbf{R}}{\mathbf{L}^{\mathsf{T}}\mathbf{L}} \tag{25}$$

Since data are sampled at a constant rate, the matrix **T** does not depend on time, the QR factorization of **T** can be calculated *a priori*. Also, notice that the coefficients in the matrix **A** do not need to be explicitly calculated. Once the estimate of the height is calculated, the wind speed vector is calculated from (4) and the ground speed vector is calculated from (2). Since this algorithm uses airspeed and optical flow information to estimate self-motion and wind speed it will henceforth be called the aero-optical egomotion estimation algorithm.

III. RESULTS

Digitized position data of a moth tracking an odor plume in a wind tunnel were used to test the algorithm. The position data were sampled at 30 Hz. Body axis orientation of the moth was also recorded. Velocity information was calculated by dividing the differential displacement in successive samples by the sampling time. Optical flow information was then simulated by dividing the velocity by the height of the moth above the floor at that instant. The optical flow information used as input to the algorithm is shown in Figure 2.

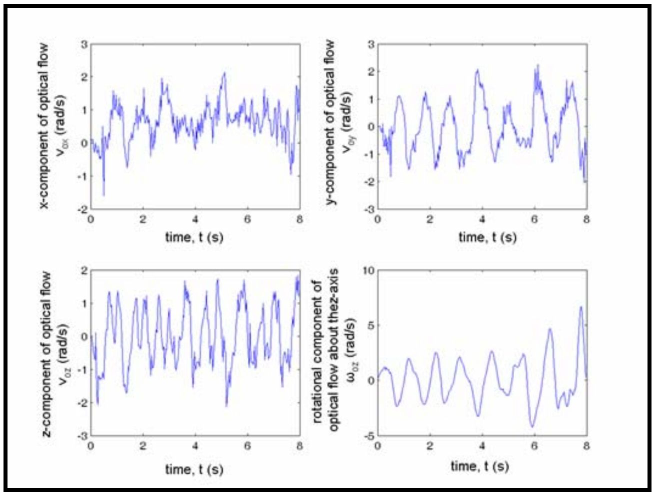

Figure 2. Optical flow data used as input to the algorithm

Wind speed data were recorded in an open field using an orthogonal set of acoustic anemometers. The wind speed data was filtered to remove noise, then resampled at 30Hz to match the sampling rate of the position data. It is assumed that no wind existed in the z-direction.

Airspeed data was simulated by subtracting the wind speed vector from the ground speed vector and adding 10% white noise. The airspeed data was simulated in this manner to test the algorithm in conditions of variable wind instead of the constant flow experienced in the wind tunnel. The airspeed data used as input to the algorithm are shown in Figure 3.

For the tests, we set n=7 and m=2. A comparison of the actual height of the moth to the estimated height of the moth as calculated by our aero-optical algorithm is shown in Figure 4. Comparisons for each component of the wind speed vector are shown in Figure 5. Comparisons for each component of the ground speed vector are shown in Figure 6. Absolute error statistics for the data in Figure 4, Figure 5, and Figure 6 are presented in Table I. An absolute error analysis was used instead of a relative error analysis because the components of wind speed and groundspeed were often near zero.

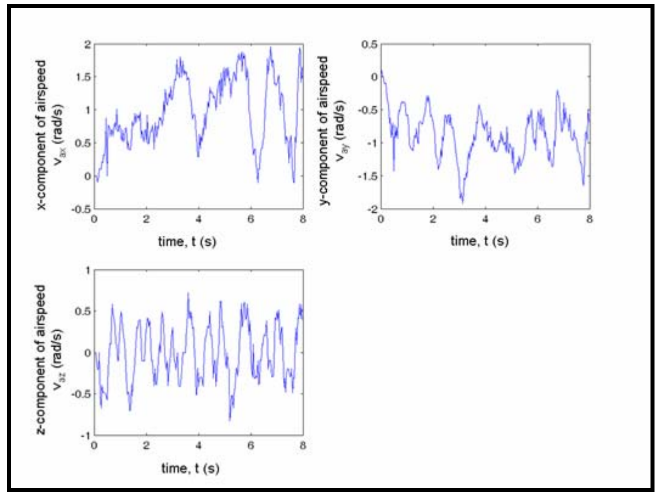

Figure 3. Airspeed data used as input to the algorithm

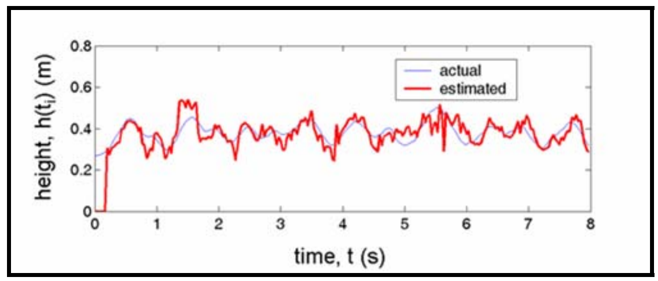

Figure 4. Comparison of the actual height of the moth to the estimated height as calculated by our aero-optical algorithm

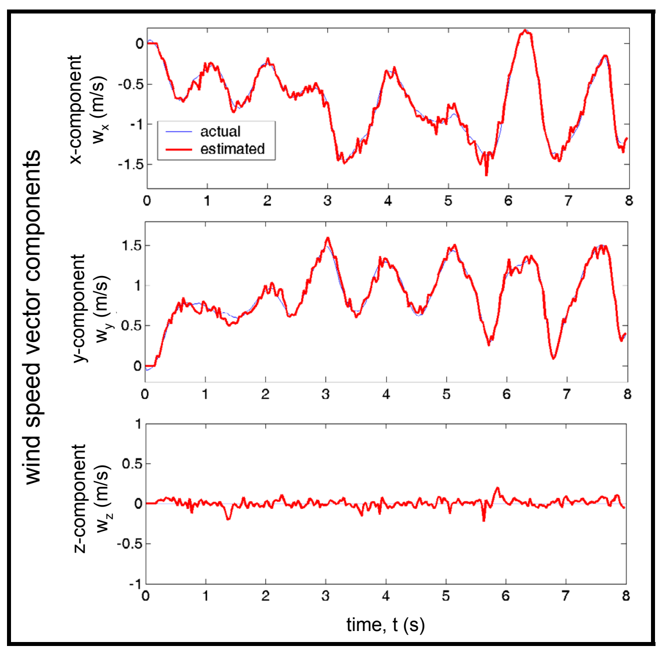

Figure 5. Comparisons of each component of the true wind speed vector to the estimates obtained using the aero-optical egomotion estimation algorithm

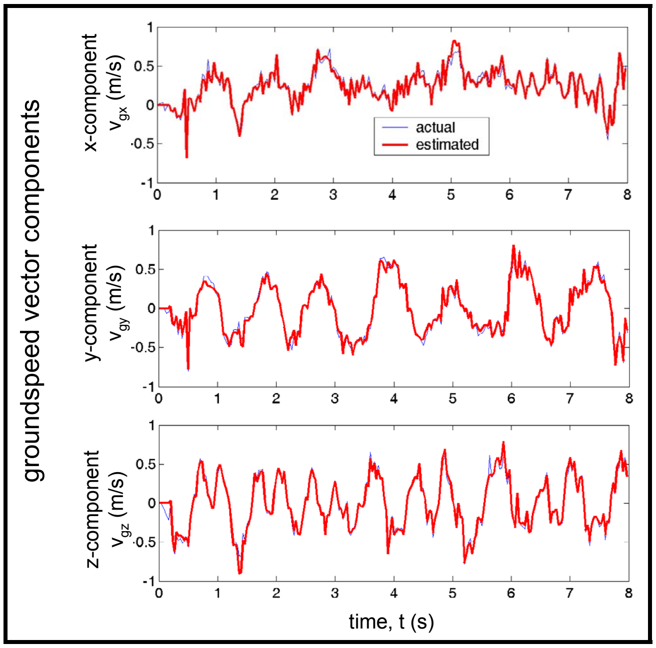

Figure 6. Comparisons of each component of the true ground speed vector to the estimates obtained using the aero-optical egomotion estimation algorithm

TABLE I. ERROR STATISTICS OF THE AERO-OPTICAL EGOMOTION ESTIMATION ALGORITHM

	mean	standard deviation
$h - \hat{h}$	0.0025 m	0.0454 m
$w_x - \hat{w}_x$	0.0087 m/s	0.0618 m/s
$w_y - \hat{w}_y$	0.0034 m/s	0.0535 m/s
$w_z - \hat{w}_z$	0.0030 m/s	0.0572 m/s
$v_{gx} - \hat{v}_{gx}$	0.0030 m/s	0.0425 m/s
$v_{gy} - \hat{v}_{gy}$	0.00004 m/s	0.0455 m/s
$v_{gz} - \hat{v}_{gz}$	0.00007 m/s	0.0428 m/s

CONCLUSIONS

The aero-optical algorithm developed in this paper was applied to moth motion data and used to accurately estimate the height and ground speed of the moth in varying wind. The algorithm was also used to estimate the wind speed. The estimate of height does not drift over time because it does not depend on previously calculated height estimates. The simulations were performed assuming level ground, but we expect that the algorithm will work on non-level ground. This needs to be demonstrated in future work.

Further statistical tests need to be performed on different data sets. The algorithm needs to be examined more closely to determine what types of data lead to less accurate estimates. Furthermore, a study should be performed to determine values for m and n that are appropriate for particular sensor data. Perhaps the values of m and n could be made adaptive to the data in such a way as to minimize the expected error between the estimate and the actual data. The algorithm will also be tested on a real mobile platform, such as Robo-Moth [13].

ACKNOWLEDGMENT

We thank Justin Bailey for providing the wind speed measurements and for his insights on current navigation technology. We thank Jenni Mueller and Jennifer Tally for their biological insights with this project. We thank Elizabeth Morrison for providing the digitized moth position and orientation data. We also thank Dr. Ravi Vaidyanathan for inspiring us to undertake this project.

REFERENCES

[1] F. A. Faruqi and K. J. Turner, "Extended Kalman Filter synthesis for integrated global positioning/inertial navigation systems", Applied Mathematics and Computation, vol. 113, 2000.

[2] A. K. Bejczy and J. Dias, "Integration of Visual and Inertial Sensors", Journal of Robotic Systems, vol. 21, January 2003.

[3] A. K. Bejczy and J. Dias, "Integration of Visual and Inertial Sensors", Journal of Robotic Systems, vol. 21, February 2003.

[4] T. S. Collett and C. J. Paterson (1991). "Relative motion parallax and target localization in the locust, *Schistocerca gragaria"*, J Comp Physiol A, vol. 169, 2000.

[5] M. V. Srinivasan, M. Poteser, and K. Kral, "Motion detection in insect orientation and navigation." Vision Research, vol. 39, 1999

[6] W. P. Chan, F. Prete, and M. H. Dickinson, Visual input to the efferent control system of a fly's "gyroscope." Science 280: 289-292. 1998

[7] A. E. Arbas, M. A. Willis, and R. Kanzaki, "Organization of goal-oriented locomotion: Pheomone-modulated flight behavior of moths," in Biological neural networks in invertebrate neuroethology and robotics, R. D. Beer, R. E. Ritzmann, and T. McKenna, Eds. San Diego: Academic Press, 1993.

[8] M. Kumon, I. Mizumoto, Z. Iwai, and M. Nagata, "Wind Estimation by Unmanned Air Vehicle with Delta Wing" Proceedings of the 2005 International Conference on Robotics and Automation, Barcelona Spain, April 2005.

[9] A. R. Ludlow, Application of Computer Modelling to Behavioral Coordination, Ph.D. thesis, University of London, 1984

[10] Snodgrass, Robert E. (1935). Principles of Insect Morphology. New York: McGraw-Hill Book Company.

[11] M. V. Srinivasan, "An image-interpolation technique for the computation of optical flow and egomotion", Biological Cybernetics, vol. 71, 1994.

[12] M. G. Nagle and M. V. Srinivasan, "Structure from motion: determining the range and orientation of surfaces by image interpolation", Journal of the Optical Society of America A, vol. 13, no. 1, January 1996

[13] A. Rutkowski, S. Edwards, M. A. Willis, R. D. Quinn, and G. C. Causey, "A Robotic Platform for Testing Moth-Inspired Plume Tracking Strategies" IEEE ICRA Conference Proceedings, 2004.